

Electronic Structure Inheritance and Pressure-Induced Polyamorphism in Lanthanide-Based Metallic Glasses

G. Li,^{1,2,*} Y. Y. Wang,¹ P. K. Liaw,² Y. C. Li,³ and R. P. Liu^{1,†}

¹State Key Laboratory of Metastable Materials Science and Technology, Yanshan University, Qinhuangdao 066004, China

²Department of Materials Science and Engineering, The University of Tennessee, Knoxville, Tennessee 37996, USA

³Beijing Synchrotron Radiation Facility, Institute of High Energy Physics, Chinese Academy of Sciences, Beijing 100039, China

(Received 6 June 2012; revised manuscript received 17 July 2012; published 18 September 2012)

We report that a series of lanthanide-based bulk metallic glasses show a pressure-induced polyamorphic phase transition observed by *in situ* angle-dispersive x-ray diffraction under high pressures. The transition started from a low-density state at lower pressures, and went through continuous densification ending with a high-density state at higher pressures. We demonstrate that, under high pressure, this new type of polyamorphism in densely packed metallic glasses is inherited from its lanthanide-solvent constituent and related to the electronic structure of $4f$ electrons. The found electronic structure inheritance could provide the guidance for designing new metallic glasses with unique functional physical properties.

DOI: 10.1103/PhysRevLett.109.125501

PACS numbers: 61.50.Ks

Being a new class of disordered materials with many attractive properties, bulk metallic glasses (BMGs) have been extensively researched on their atomic structures and relationships to properties. Despite the chemical and structural complexity of BMGs, more and more researchers suggest that the short-range order (SRO) is characterized by solute-centered clusters, each of which is made up of a solute atom surrounded by a majority of solvent atoms, and the medium-range order (MRO) is constructed by packing of the clusters beyond the SRO [1–3]. Recently, Ma *et al.* and Wang [4,5] revealed that the more compliant solvent-solvent bonds are sustaining the majority of strains upon deformation, and the mechanical properties are dominated by the solvents in BMGs. This feature invites the question: would a solvent's electronic structural properties be inherited in its same component-bearing BMGs? Lanthanide-based BMG systems have special electronic structures, which are characterized by a gradual filling of the $4f$ shell. Lanthanides elements are in the same location and exhibit chemical and structural similarity [6]. When electrons are added to these atoms, the atomic number is increased normally to go into the $4f$ shells, which are interior to the atoms, and thus do not change the bulk properties of the metals. However, if the atoms are brought closer together at high pressures, this behavior will be modified. Most substances exhibit structure change under high pressures [7,8]. Research on electronic interactions [9] and atomic volumes [10] in rare-earth metals at high pressures have confirmed that there are a great number of crystalline polymorphic transitions in pure elemental rare-earth metals and related alloys and compounds for the strongly correlated $4f$ electrons of the rare-earth metals. Therefore, rare-earth-based BMGs are an ideal model system for studying the electronic-structural inheritance in BMGs. Recently, the pressure-induced transition between two amorphous phases in the Ce-based BMGs [10,11], $(La_{0.5}Ce_{0.5})_{64}Al_6Ni_5Cu_{15}$

[12], $La_{68}Al_{10}Cu_{20}Co_2$, and $Nd_{60}Al_{10}Ni_{10}Cu_{20}$ [13] in atomic percent (at. %) have been reported. Using x-ray absorption spectroscopy, the gradual and continuous delocalization of $4f$ electrons under high pressures was observed in the $Ce_{75}Al_{25}$ binary metallic glass [14]. However, the reasons for the polymorphic transitions under high pressures remain unclear. It is intriguing to see if this kind of polyamorphic transition occurs in other lanthanide-based BMG systems.

In this Letter, we focus on the compressive behavior of Gd- and Pr-based BMGs under high pressures by *in situ* angle-dispersive x-ray diffraction (ADXRD) with a synchrotron radiation source. The purpose is to study the effect of lanthanide solvent-component electronic states on their BMG structural inheritance and pressure-induced polyamorphic transitions in lanthanide-based BMGs. Our results provide evidence for the electronic-structural inheritance in metallic glasses, which might be important for understanding the structure and the polyamorphism in BMGs and helpful for designing new BMGs with unique properties.

The preparation of $Gd_{40}Y_{16}Al_{24}Co_{20}$ and $Pr_{60}Cu_{20}Al_{10}Ni_{10}$ BMGs in at. % can be found in Refs. [15,16]. Some powders were carefully scraped by the 4Cr13 stainless-steel scalpel from both of the amorphous rods for pressure experiments. The amorphous nature of the scraped powders is confirmed by x-ray diffraction (XRD). The pressure was generated using a diamond anvil cell. The culet of the diamond anvil is 400 μm in diameter. The amorphous powder sample together with the pressure-calibrator ruby was loaded into a 120 μm -diameter hole of a T301 stainless-steel gasket, which was preindented to a thickness of about 40 μm . Silicone oil was used as the pressure-transmitting media. The *in situ* ADXRD measurements were carried out in the Beijing Synchrotron Radiation Laboratory. The Debye rings were recorded using an image plate in a transmission mode, and the XRD patterns were

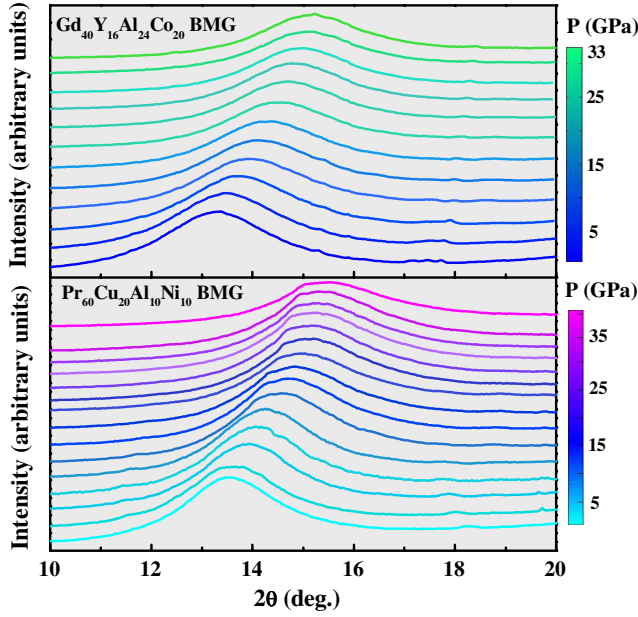


FIG. 1 (color online). Synchrotron radiation x-ray diffraction spectrum of $\text{Gd}_{40}\text{Y}_{16}\text{Al}_{24}\text{Co}_{20}$ and $\text{Pr}_{60}\text{Cu}_{20}\text{Al}_{10}\text{Ni}_{10}$ BMGs.

integrated from the images using the FIT2D software [17]. The size of the x-ray spot was $45 \times 26 \mu\text{m}^2$. A Li detector was used to collect the diffraction signal under various pressures. The experimental pressure was determined from the position of the diffraction peak of ruby.

Synchrotron radiation x-ray diffraction spectra under different pressures of Gd- and Pr-based BMGs are shown in Fig. 1. With the increase of the pressure, the broad diffusive amorphous halo obviously shifts to a higher wave vector due to the compression effect. No sharp Bragg peaks are detected at the applied pressures, which mean that the samples' glassy natures are quite stable at room temperature.

The first halo in the above patterns referring to the first sharp diffraction peak (FSDP) reveals the structural information of the medium-range length scale in BMGs [3]. The position of the FSDP, q_1 (q is the momentum transfer, $q = 4\pi \sin\theta/\lambda$, where 2θ is the diffraction angle, and λ is wavelength), characterizes the medium-range correlation. The scaling of the FSDP (q_1) in metallic glasses comes from the MRO [4], and the structure factor, $S(q_1)$, obtained by the program PDF get N [18], is more efficient in response to MRO in BMGs [4,19–22]. Therefore, we analyze the difference of the total structure factors, $\Delta S_p(q_1)$, upon the applied pressures to see if there exists an amorphous-amorphous phase transition in BMGs. While $\Delta S_p(q_1) = S_p(q_1) - S_0(q_1)$, $S_0(q_1)$ corresponds to the FSDP position of BMGs in the ambient-pressure XRD data, $S_p(q_1)$ refers to those of the applied pressures. The differences of $S_p(q_1)$ under high pressures are shown in Fig. 2. The changes indicate that the structure does exist differently between its initial configuration under high

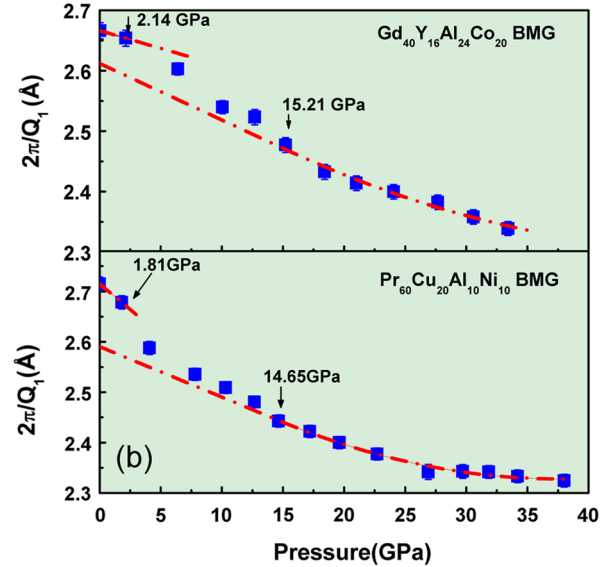
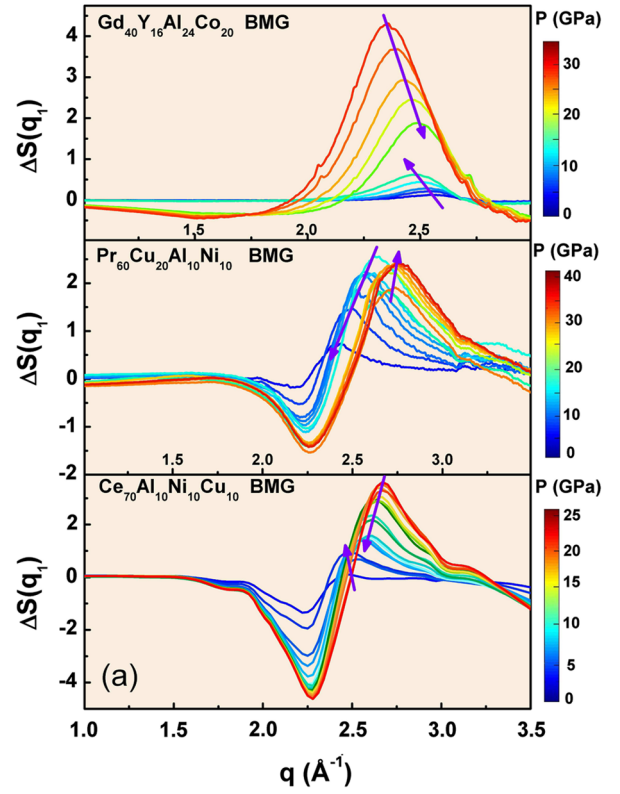


FIG. 2 (color online). (a) The difference plot of $\Delta S(q_1)-q$ for $\text{Gd}_{40}\text{Y}_{16}\text{Al}_{24}\text{Co}_{20}$, $\text{Pr}_{60}\text{Cu}_{20}\text{Al}_{10}\text{Ni}_{10}$, and $\text{Ce}_{70}\text{Al}_{10}\text{Ni}_{10}\text{Cu}_{10}$ BMGs (data of $\text{Ce}_{70}\text{Al}_{10}\text{Ni}_{10}\text{Cu}_{10}$ BMG were taken from Ref. [12] and calculated using the program of Ref. [18]). (b) Inverse FSDP positions $2\pi/Q_1-P$ of $\text{Gd}_{40}\text{Y}_{16}\text{Al}_{24}\text{Co}_{20}$ and $\text{Pr}_{60}\text{Cu}_{20}\text{Al}_{10}\text{Ni}_{10}$ BMGs.

pressures. The pressure dependence of the $S_p(q_1)$, expressed by $\Delta S(q_1)$, changes twice over the slope (as the arrow shows) between 2.14 and 33.42 GPa for the $\text{Gd}_{40}\text{Y}_{16}\text{Al}_{24}\text{Co}_{20}$ BMG, and between 1.81 GPa and 42.06 GPa for the $\text{Pr}_{60}\text{Cu}_{20}\text{Al}_{10}\text{Ni}_{10}$ BMG in Fig. 2(a).

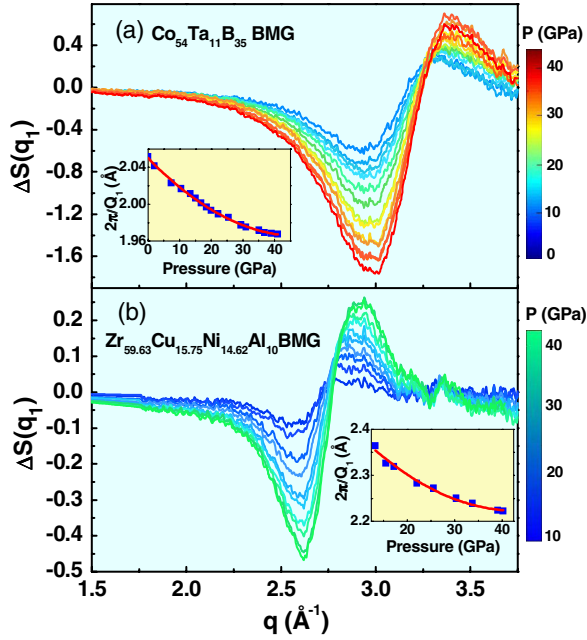


FIG. 3 (color online). $\Delta S(q_1)$ - q and $2\pi/Q_1$ - P curves of (a) Co-based and (b) Zr-based BMG (Co-based data were taken from our previous result in Ref. [24], while Zr-based BMG is from Ref. [25]).

This indicates at least two different amorphous phases existing in the applied pressure range: low- and high-density states, in line with three pressure ranges of different densities defined solely from the data of the inverse FSDP positions, $2\pi/Q_1$, of the two BMGs as a function of pressure shown in Fig. 2(b), discussed below.

In Fig. 2(b), two distinct states can be identified, the low-density area and high-density area (dashed red line), along with a transition region from about 2.14 to 15.21 GPa for $\text{Gd}_{40}\text{Y}_{16}\text{Al}_{24}\text{Co}_{20}$ and 1.81 to 14.65 GPa for $\text{Pr}_{60}\text{Cu}_{20}\text{Al}_{10}\text{Ni}_{10}$ BMGs. In Ce-based BMGs polyamorphic transitions [11,12], the difference of $S_p(q_1)$ under high pressures is shown in Fig. 2(a), the pressure dependence of $\Delta S(q_1)$ also changes twice over the slope, which is similar to the shape as that of Pr- and Gd-based BMGs in Figs. 2(a). This trend further confirms the polyamorphic transitions in our Gd- and Pr-based BMGs. In Co- and Zr-based BMGs, there are no $4f$ electrons in solvent elements, Co and Zr. The $\Delta S(q_1)$ - q and $2\pi/Q_1$ - P plots of the two BMGs as a function of pressure are shown in Fig. 3. The $\Delta S(q_1)$ - q curves keep an unchanged slope. The $2\pi/Q_1$ - P curves change smoothly, and the volume-pressure relationship of both Co- and Zr-based BMGs can be well fitted by the Bridgman equation of state [23–25], which means no amorphous-to-amorphous or amorphous-to-crystalline phase transitions upon the applied pressures. To further confirm our claim, we focus on quantitative analysis on FSDP, transformed by the high-angle diffraction patterns. According to Figs. 2 and 3, we noted that upon the experimental pressures, q_1 increases from 2.25 to 2.74 (by $\sim 22\%$) for the Pr-based

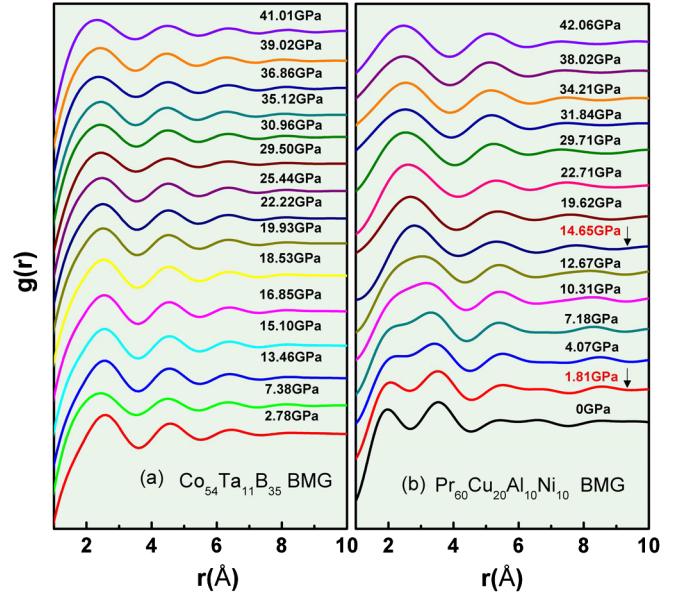


FIG. 4 (color online). Pair distribution functions, $g(r)$, of (a) $\text{Co}_{54}\text{Ta}_{11}\text{B}_{35}$ BMG and (b) $\text{Pr}_{60}\text{Cu}_{20}\text{Al}_{10}\text{Ni}_{10}$ BMG.

BMG, 2.35 to 2.68 (by $\sim 14\%$) for the Gd-based BMG, and 2.32 to 2.64 (by $\sim 13\%$) for the Ce-based BMG, while 3.05 to 3.22 (by $\sim 5.2\%$) for the Co-based BMG, and 2.58 to 2.73 (by $\sim 5.8\%$) for the Zr-based BMG. For the Gd- and Pr-based BMGs with polyamorphic transitions, the difference in q_1 is almost 3 times greater than the BMGs without phase transformation. As shown is Fig. 4, we also investigate the $g(r)$ - r relationship of the Co-based BMG and Pr-based BMG under selected pressures. For the Co-based BMG, upon the applied pressures, the shapes of the $g(r)$ - r remain unchanged, which means the Co-based BMG retains its glassy structure up to 41 GPa. But for the Pr-based BMG, the $g(r)$ - r relationship shows three parts: 0–1.81 GPa, 4.07–12.67 GPa, and larger than 14.65 GPa, which corroborates with Fig. 2(b) very well. This trend confirms that the glassy structure changed from ambient to high pressures. These results suggest that complex $4f$ electrons result in a polyamorphic transition in the lanthanide BMGs.

We check the phase change under high pressures for $\text{Mg}_{65}\text{Cu}_{25}\text{Tb}_{10}$ BMGs with the $4f$ electrons state lanthanide component, Tb, but the lanthanide component, Tb, is not the solvent element. Even though there is a Tb component $4f^9$ electrons state, but with only 10 at. % Tb, not being a solvent element in the BMG, our previous research has confirmed that, at room temperature, no phase transition occurs up to 31.19 GPa [26]. But the $\text{Ce}_{32}\text{La}_{32}\text{Al}_{16}\text{Ni}_{15}\text{Cu}_5$ BMG has phase-transition solvent elements, Ce and La, which atomic component sums to 64 at.%, and has also been confirmed to have the amorphous-amorphous phase transition [14]. Here we draw a conclusion that the polyamorphic transition in the lanthanide BMGs inherits from solvent component's crystalline polymorphic transitions related to the $4f$ electronic state.

TABLE I. Contrast of the behavior under high pressures of Ce-, Gd-, and Nd-based BMGs and related rare-earth components at room temperature.

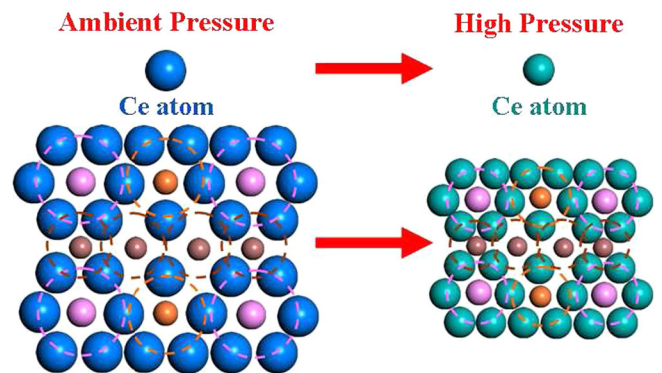
Materials	Phase transition pressure (GPa)	Reference
Ce ₅₅ Al ₄₅ BMG	2.0, 13.5	[2]
Ce ₇₅ Al ₂₅ BMG	1.5, 5	[11]
Ce ₇₀ Al ₁₀ Ni ₁₀ Cu ₁₀ BMG	2.0, 10	[12]
Ce	0.75, 0.9, 5.0, 1.5	[6,12,27,28]
Gd ₄₀ Y ₁₆ Al ₂₄ Co ₂₀ BMG	2.14, 15.21	This work
Gd	12.5, 20.6, 20–25	[29,9]
Pr ₆₀ Cu ₂₀ Al ₁₀ Ni ₁₀ BMG	1.81, 14.65	This work
Pr	4	[9]
Nd ₆₀ Al ₁₀ Ni ₁₀ Cu ₂₀ BMG	1.17	[13]
Nd	5.0	[9]
(La _{0.5} Ce _{0.5}) ₆₄ Al ₆ Ni ₅ Cu ₁₅ BMG	14	[14]

Table I gives the contrast of the behavior under high pressures of the solvent components pure rare-earth metals and BMGs. All the metallic components, Ce, Nd, Pr, and Gd, have phase transition under high pressures [30,27,28], and their corresponding BMGs also exhibit the amorphous-to-amorphous phase transition. Take Ce, for example, whose phase transition stems from the $4f$ electrons' strong correlation [31,32].

The $4f^1$ component basically is a pure localized $4f$ configuration. During compression, the postedge feature, denoted itinerant $4f^0$ [33,34], appeared at about 10 eV higher energy than the $4f^1$ feature and grew with increasing the pressure, while the intensity of the $4f^1$ component decreased. Considering that the electronic shells of Ce ($4f^1 5d^1 6s^2$), Pr ($4f^3 5d^1 6s^2$), Nd ($4f^4 5d^1 6s^2$), and Gd ($4f^7 5d^1 6s^2$) are similar, and only the electron number is different in the $4f$ shell, we suggest that the $4f^n$ (n is from 1–7) component basically is a pure localized $4f$ configuration; that is to say, for Pr, it is $4f^3$, Gd is $4f^7$, and Nd is $4f^4$. With increasing pressure, $4f^0$ increases, the ratio of higher energy components, $4f^0$ to $4f^1$, increased continuously over the intermediate region (usually in lower pressures) and reached a plateau above higher pressures [11]. This trend clearly demonstrates the gradual and continuous delocalization of $4f$ electrons under high pressures, and coincides with the volume collapse shown in Fig. 2(b) under the lower pressure range of 2.14 to 15.21 GPa for Gd-based BMG and 1.81 to 14.65 GPa for Pr-based BMG. Table I suggests that the inheritance of the change of the solvent metallic $4f$ electronic state is essentially responsible for the amorphous-to-amorphous phase transition in BMGs. Why do solvent components have such important effects on their glassy-alloy state? Polyamorphism is dictated by the Ce $4f$ electronic transition from the localized to itinerant state. This is fundamentally different from the standard structural polyamorphism, which is dictated by coordination changes and topological rearrangements of atoms. The electrical-properties inheritance is useful for searching for polyamorphism in other metallic glasses,

which contain other f metals with possible localized-itinerant electron transitions or unique physical properties.

Research on Ce pure metal shows that, at room temperature, when pressure is applied around 0.9 GPa, the face-centered-cubic (fcc) isostructural γ - α phase transition sharply occurs, accompanied with a decrease in the volume of 15% [12], in which all Ce atoms have identical local environments and transform in unison. While in the lanthanide BMGs, each lanthanide atom encounters random and different local environments and transforms differently over a pressure range. As shown in Fig. 5, in the long-range order (LRO) pure lanthanide crystalline metal, isostructural phase transition occurs, which $4f^n$ (the biggest size balls in the figure) sharply transforms into $4f^0$ (the biggest size balls) under high pressures. Lacking the long-range crystalline order in lanthanide BMGs, SROs are characterized by solute-centered clusters, each of which is made up of a solute atom surrounded by a majority of solvent atoms [1–3]. The transformation of $4f^n$ to $4f^0$ only takes place in solvent atoms. The solvent atoms surround other solute atoms, and all those solute atoms are without $4f$ electron transitions. Therefore, in spite of the “color” change, the lanthanide BMGs are still in their origin of MRO but no LRO.

FIG. 5 (color online). Schematic illustration of phase transition in metallic glasses related to the $4f$ electronic state.

In summary, we demonstrate that the polyamorphous transition in lanthanides BMGs upon applying a pressure is related to the amorphous-to-amorphous transition of the solvent component in glassy alloys. Lanthanides BMGs all exhibit three different amorphous regions upon the application of pressures. A low-density state is observed at ambient conditions, which becomes a higher-density state, while pressure is increased. An intermediate region shows a gradual transition. For lanthanide BMGs, their polyamorphization under high pressures is closely related to the behavior of $4f$ electrons in solvent metals.

This work was supported by the National Basic Research Program of China (Grant No. 2010CB731600) and National Science Foundation of China (Grant No. 50731005/51121006). P.K. Liaw very much appreciates the U.S. National Science Foundation (DMR-0909037, CMMI-0900271, and CMMI-1100080).

*Corresponding author.
gli25@utk.edu

†Corresponding author.
riping@ysu.edu.cn

- [1] D. B. Miracle, *Nature Mater.* **3**, 697 (2004).
- [2] H. W. Sheng, W. K. Luo, F. M. Alamgir, J. M. Bai, and E. Ma, *Nature (London)* **439**, 419 (2006); H. W. Sheng, H. W. Sheng, H. Z. Liu, Y. Q. Cheng, J. Wen, P. L. Lee, W. K. Luo, S. D. Shastri, and E. Ma, *Nature Mater.* **6**, 192 (2007).
- [3] D. Ma, A. D. Stoica, and X. L. Wang, *Nature Mater.* **8**, 30 (2008).
- [4] D. Ma, A. D. Stoica, X.-L. Wang, Z. P. Lu, B. Clausen, and D. W. Brown, *Phys. Rev. Lett.* **108**, 085501 (2012).
- [5] W. H. Wang, *Nature Mater.* **11**, 275 (2012).
- [6] J. F. Cannon, *J. Phys. Chem. Ref. Data* **3**, 781 (1974).
- [7] S. Merkel *et al.*, *Science* **311**, 644 (2006).
- [8] H. K. Mao, J. F. Shu, G. Y. Shen, R. J. Hemley, B. Li, and A. K. Singh, *Nature (London)* **399**, 280 (1999).
- [9] W. H. Gust and E. B. Royce, *Phys. Rev. B* **8**, 3595 (1973).
- [10] W. A. Grosshans and W. B. Holzapfel, *Phys. Rev. B* **45**, 5171 (1992).
- [11] Q. S. Zeng, Y. Ding, W. L. Mao, W. Yang, J. Shu, S. V. Sinogeikin, H.-k. Mao, and J. Z. Jiang, *Phys. Rev. Lett.* **104**, 105702 (2010).
- [12] M. J. Duarte, P. Bruna, E. Pineda, D. Crespo, G. Garbarino, R. Verbeni, K. Zhao, W. H. Wang, A. H. Romero, and J. Serrano, *Phys. Rev. B* **84**, 224116 (2011).
- [13] X. R. Liu and S. M. Hong, *Appl. Phys. Lett.* **90**, 251903 (2007).
- [14] Q. S. Zeng *et al.*, *Proc. Natl. Acad. Sci. U.S.A.* **104**, 13565 (2007).
- [15] B. Zhang, D. Q. Zhao, M. X. Pan, W. H. Wang, and A. L. Greer, *Phys. Rev. Lett.* **94**, 205502 (2005).
- [16] Z. F. Zhao, Z. Zhang, P. Wen, M. X. Pan, D. Q. Zhao, W. H. Wang, and W. L. Wang, *Appl. Phys. Lett.* **82**, 4699 (2003).
- [17] A. P. Hammersley, S. O. Svensson, M. Hanfland, A. N. Fitch, and D. Hausermann, *High Press. Res.* **14**, 235 (1996).
- [18] P. F. Peterson, M. Gutmann, Th. Proffena, and S. J. L. Billinge, *J. Appl. Crystallogr.* **33**, 1192 (2000).
- [19] Y. Suzuki, J. Haimovich, and T. Egami, *Phys. Rev. B* **35**, 2162 (1987).
- [20] G. S. Cargill, III, *Solid State Phys.* **30**, 227 (1975).
- [21] C. Fan, P. K. Liaw, and C. T. Liu, *Intermetallics* **17**, 86 (2009); C. Fan, H. G. Yan, C. T. Liu, H. Q. Li, P. K. Liaw, Y. Ren, and T. Egami, *Intermetallics* **23**, 111 (2012).
- [22] C. Fan, P. K. Liaw, T. W. Wilson, W. Dmowski, H. Choo, C. T. Liu, J. W. Richardson, and Th. Proffen, *Appl. Phys. Lett.* **89**, 111905 (2006).
- [23] P. W. Bridgman, *The Physics of High Pressure* (Bell, London, 1958).
- [24] J. F. Wang *et al.*, *Appl. Phys. Lett.* **99**, 151911 (2011).
- [25] G. Li, Q. Jing, T. Xu, L. Huang, R. P. Liu, and J. Liu, *J. Mater. Res.* **23**, 2346 (2008).
- [26] G. Li, Y. C. Li, Z. K. Jiang, T. Xu, L. Huang, J. Liu, T. Zhang, and R. P. Liu, *J. Non-Cryst. Solids* **355**, 521 (2009).
- [27] E. Franceschi and G. L. Olcese, *Phys. Rev. Lett.* **22**, 1299 (1969).
- [28] D. B. McWhan, *Phys. Rev. B* **1**, 2826 (1970).
- [29] D. B. McWhan and A. L. Stevens, *Phys. Rev.* **139**, A682 (1965).
- [30] P. W. Bridgman, *Physics of High Pressures* (Bell, London, 1952).
- [31] P. Soderlind, *Adv. Phys.* **47**, 959 (1998).
- [32] A. B. Shick, W. E. Pickett, and A. I. Liechtenstein, *J. Electron Spectrosc. Relat. Phenom.* **114-116**, 753 (2001).
- [33] J. P. Rueff, C. F. Hague, J.-M. Mariot, L. Journel, R. Delaunay, J.-P. Kappler, G. Schmerber, A. Derory, N. Jaouen, and G. Krill, *Phys. Rev. Lett.* **93**, 067402 (2004).
- [34] J. P. Rueff, J.-P. Itié, M. Taguchi, C. F. Hague, J.-M. Mariot, R. Delaunay, J.-P. Kappler, and N. Jaouen, *Phys. Rev. Lett.* **96**, 237403 (2006).